Wave Direction Estimation Based on Local Gradient Techniques from Satellite Imagery for Coastal Dynamics Monitoring

Woramet Simrum* Paweena Kanokhong* Chakapat Chokchaisiri* Somrudee Deepaisarn*
Kittipisut Chansri† Chanyut Lisawat† Waranrach Viriyavit†
Akkharawoot Takhom‡ Phutphalla Kong§ Didin Agustian Permadi¶ Sharifah Hafizah Syed Ariffin‖
Surasak Boonkla** Kasorn Galajit** and Jessada Karnjana**
* Sirindhorn International Institute of Technology, Thammasat University, Pathum Thani, Thailand
E-mail: {6422771400, 6422800126, m6622040308}@g.siit.tu.ac.th, somrudee@siit.tu.ac.th
† Burapha University, Thailand
E-mail:{66160292, 66160295, waranrach.vi}@go.buu.ac.th
‡ Faculty of Engineering, Thammasat University, Thailand
E-mail: takkhara@tu.ac.th
§ Cambodia Academy of Digital Technology, Cambodia
E-mail: phutphalla.kong@cadt.edu.kh
¶ Environmental Engineering, Institut Teknologi National Bandung, Indonesia
E-mail: didin@itenas.ac.id
‖ Universiti Teknologi Malaysia, Malaysia
E-mail: shafizah@utm.my
** NECTEC, National Science and Technology Development Agency, Pathum Thani, Thailand
E-mail: {surasak.boonkla, kasorn.galajit, jessada.karnjana}@nectec.or.th

***Abstract*—This paper proposes a wave direction estimation method using high-resolution satellite image patches to support coastal dynamics analysis, providing greater insight into coastal erosion and make coastal management more effective. The method draws inspiration from local gradient techniques used in SAR-based wind retrieval but adapts them to optical imagery with a more straightforward implementation. Using Sobel filters, dominant wave crest orientations are extracted from each image patch. After noise removal via thresholding and median filtering, wave direction is computed from edge orientations using a double-angle trigonometric averaging approach. Experiments on Thailand's coastal imagery demonstrate that the method produces robust average wave direction estimates at patch scale, offering a scalable and approach to wave pattern analysis without additional instrument installation. The experimental results show a mean absolute error (MAE) of 6.9 degrees and a root mean square error (RMSE) of 8.3 degrees, indicating a high level of agreement between the estimated and reference wave directions. Furthermore, 89.5 percent of the predictions fall within plus or minus 15 degrees of the reference values. However, the accuracy of method depends on image quality and parameter tuning, highlighting the need for consistent preprocessing.**

I. Introduction

Coastal erosion circumstance refers to the process by which shorelines are gradually eroded due to natural forces such as waves, currents, tides, and wind, as well as human-induced activities such as coastal development and sand mining [1], [2]. In Thailand, this phenomenon has become increasingly significant, particularly along low-lying, sediment-rich coasts such as those of the Gulf of Thailand and the Andaman sea [3], [4].

The impacts of coastal erosion extend beyond the physical land loss, affecting both local economies and local communities [4]. Coastal infrastructure, tourism, and agriculture are affected, while the displacement of residents and the degradation of natural ecosystems worsen their socioeconomic vulnerability [5]. Notably, in areas like Bangsaen beach and Songkhla lake, erosion has led to the loss of recreational spaces and reduced safety due to dangerous rip currents [6], [7].

To mitigate these effects, various protection strategies have been implemented, including hard structures such as seawalls, breakwaters, and groins, as well as soft measures like beach nourishment and mangrove planting [5], [8]. These protective structures aim to reduce wave energy and sediment transport, thus stabilizing the shoreline [4], [8].

However, while these interventions can temporarily slow erosion, they are not always successful in the long term and can sometimes cause unintended negative consequence [7]. For example, installing breakwaters can shift erosion to adjacent, unprotected areas or interfere with natural sediment flows [2], [5]. Even after such structures are built, studies still report ongoing shoreline retreat in various locations [6]. This reveals the need for more adaptive and informed coastal management strategies. To improve the effectiveness of protection and prevention measures, it is essential to study the underlying causes of coastal erosion, particularly the dynamic interac-

979-8-3315-7206-8/25/$31.00

tions between physical and environmental forces [2], [3]. Key contributing factors include wave direction and height, wind patterns, tides, sediment supply, and coastal currents [1], [2].

Wave direction, in particular, plays a critical role in determining sediment transport patterns and beach morphology [2]. Wave direction is a critical parameter in coastal monitoring, hazard assessment, and marine infrastructure design. Conventionally, wave direction in offshore regions is estimated using oceanographic instruments such as wave rider buoys, floating sensor nodes, high frequency radar systems, and satellite altimeters [9], [10], [11]. These methods provide reliable measurements but often involve high costs, sparse spatial coverage, and maintenance challenges, especially in deep sea or remote areas.

In contrast, nearshore wave direction estimation remains more limited, primarily due to complex bathymetry, wave breaking, and interaction with coastal features. While some nearshore stations exist, they are sparse and typically rely on fixed-point measurements [12], [13]. Moreover, remote sensing approaches such as synthetic aperture radar (SAR) and video-based shoreline monitoring have been explored, but most require specialized platforms or complex calibration.

Although several studies use satellite images to analyze coastal changes and morphology, such as in Songkhla, Phuket, and Phetchaburi, there is a noticeable gap in the literature when it comes to directly estimating wave direction from satellite imagery [3], [4], [5]. In recent years, the monitoring of coastal dynamics has increasingly relied on satellite imagery, which enables large-scale, long-term observation of shoreline change. This represents a shift away from conventional approaches that depend on real-time hydrodynamic parameters such as wave direction and current velocity [14].

Therefore, to enhance the ability to predict and manage coastal erosion in Thailand, we explore methods that can estimate wave direction directly from satellite images. Such approaches would enable more efficient and large-scale monitoring of coastal dynamics and support the development of better-informed protective strategies.

Traditional approaches for estimating wave direction, such as directional wave spectrum analysis [15], [16], have long been used to study the wave energy distribution in different directions. However, these methods focus primarily on energy spectra rather than providing spatially detailed wave direction information. Geometric and physical models have also been employed to estimate the direction of the wave based on the shape of wave crests, but their effectiveness is often limited by the need for in situ measurements [17]. Furthermore, wave-driven sediment transport models provide valuable insights into sediment movement but rely heavily on accurate wave direction data, which remains a challenge for complex coastal environments [18].

In this study, we propose an improved method for estimating wave direction from satellite images by adapting the concept of the local gradient method originally developed for the estimation of wind direction [19]. The proposed solution adapts the local gradients method introduced by Koch (2004), originally designed for wind direction retrieval from SAR imagery [19]. By modifying and optimizing this algorithm, we aim to estimate the wave direction instead of the wind direction, using high-resolution satellite imagery. This adaptation is expected to provide more spatially detailed and localized wave direction data than existing interpolation-based methods, and it may serve as a foundation for real-time coastal dynamic monitoring and erosion risk prediction. The main objective of this proposed method is to increase the accuracy and robustness of wave direction estimation by addressing some inherent limitations of previous techniques. Specifically, we extend the local gradient method to better handle noise, edge detection, and the ambiguity of wave direction, especially in the presence of complex coastal environments.

Coastal erosion is a shared concern among ASEAN countries due to similar geographic and environmental conditions. To address this challenge, we initiated a collaborative research project among four ASEAN countries (Thailand, Indonesia, Malaysia, and Cambodia) and Japan under the ASEAN IVO framework. This study contributes to that effort by exploring satellite-based approaches that can support regional coastal monitoring and management.

The remainder of this paper is organized as follows. Section 2 describes the satellite data sources, image preprocessing steps, and dataset construction process. Section 3 presents the proposed method for estimating wave direction. Section 4 outlines the experimental setup, evaluation metrics used to assess the performance of the method, and experimental results. Section 5 discusses the results and their implications for coastal monitoring applications. Section 6 concludes the paper by summarizing the key findings and proposing directions for future research.

II. Dataset Construction

This section outlines the process of preparing satellite imagery and constructing the wave direction dataset. The methodology includes image acquisition, patch generation, and manual wave direction annotation, forming the basis for coastal wave pattern analysis.

A. Image Acquisition

High-resolution satellite images of the coastal regions, specifically Sattahip beach (Sattahip district, Chonburi province) and Chaloem Burapha Chonlathit road (Laem Sing district, Chanthaburi province) were captured using Google Earth Pro. Each image was taken from a top-down perspective aligned to true north with 12 o'clock orientation, ensuring consistent directional reference across samples. The eye altitude varied between 600 meters, 800 meters, and 1000 meters to balance detail resolution and spatial coverage. All images were exported at 8K resolution to maintain visual clarity of the wave crest patterns.

B. Patch Generation

To facilitate localized analysis of wave directions, each satellite image was divided into smaller patches measuring 244 × 244 pixels using a sliding window approach. Two methods were employed as follows. First, random sampling was employed, in which 300 patches were randomly selected from a grid-based slicing of the image. Second, full grid-based slicing was used, where all non-overlapping patches from the entire image were retained. These patches allowed for focused, small- scale inspection of wave patterns, as shown in Fig. 1.

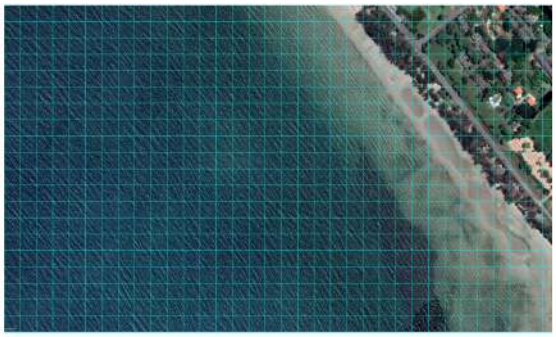

Fig. 1. Original image with 244×244 grid overlay.

C. Wave Direction Annotation

Each patch was manually labeled using GIMP. The measure tool was used to draw a line perpendicular to the wave crest, always directed vertically upward in alignment with the north-up image orientation. GIMP displayed the angle between the drawn line and the vertical axis. Since GIMP reports only positive values, manual interpretation was applied. For example, a left-tilted wave crest was recorded as a negative angle with respect to the north, e.g., $-74.07°$. A right-tilted wave crest was recorded as a positive angle, e.g., $+23.46°$, as shown in Fig. 2.

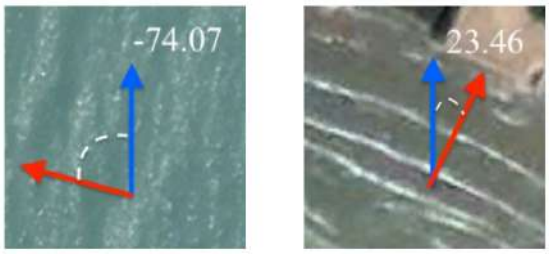

Fig. 2. Visualization of the wave direction annotation, with directional arrows overlaid on the satellite image patch.

A horizontal wave crest, regardless of direction, was recorded as $90°$. Each annotated sample was recorded in a structured CSV file, with entries including patch ID, source image reference, and wave direction angle. This process yielded over 600 labeled patches, combining both sampling strategies.

III. Proposed Method

Our method operates through a series of preprocessing, gradient computation, noise reduction, and directional averaging steps. By combining these steps, we enhance the quality of the satellite image and improve the estimation of wave direction in various coastal regions of Thailand. The following is a breakdown of the four steps in the proposed method.

A. Image Loading and Preprocessing

Satellite images are often affected by lighting inconsistencies and contrast variations due to atmospheric conditions and sensor limitations. To enhance wave pattern clarity and ensure reliable edge detection, three preprocessing steps are applied as follows.

First, the input color image is converted to grayscale, transforming it into a single-channel representation. This process focuses on intensity variations rather than color information, which is essential for accurate edge detection.

Second, histogram equalization is applied to enhance image contrast by redistributing pixel intensity values to approximate a uniform distribution [20]. This step is particularly effective for images where wave patterns are not easily distinguishable due to low contrast.

$$s_k = \left\lfloor (L-1) \sum_{j=0}^{k} \frac{n_j}{N} \right\rfloor, \tag{1}$$

where s_k is the new intensity value, L is the total number of intensity levels (typically 256), k represents the current intensity level being processed in the histogram equalization algorithm, n_j is the number of pixels with intensity j, and N is the total number of pixels.

Last, to reduce high-frequency noise while preserving edge structures, Gaussian smoothing is applied using a 5×5 kernel with the mean of 0 ($\mu = 0$) and the variance of 1.21 ($\sigma^2 = 1.21$). This method effectively balances noise reduction and detail preservation.

B. Image Enhancement and Filtering

After preprocessing, we compute the image gradients using the Sobel operator [21]. These gradients provide critical directional information to estimate the orientation of wave patterns. The process consists of four subprocesses as follows.

First, the Sobel operator is used to calculate the image gradients along the horizontal (x) and vertical (y) directions. This method is chosen for its simplicity and effectiveness in detecting directional intensity changes.

$$G_x = \frac{\partial I}{\partial x}, \quad \text{and} \quad G_y = \frac{\partial I}{\partial y}, \tag{2}$$

where I denotes the image intensity, G_x and G_y represent the gradient components in the horizontal and vertical directions, respectively, and x and y are the spatial coordinates corresponding to the image's horizontal (column-wise) and vertical (row-wise) axes.

Second, the gradient magnitude and direction are determined using following equations.

$$M = \sqrt{G_x^2 + G_y^2}, \tag{3}$$

and

$$\theta_{x,y} = \arctan\left(\frac{G_y}{G_x}\right), \tag{4}$$

where M represents the strength of the gradient (or edge) at a given point, $\theta_{x,y}$ represents the orientation (angle) of the gradient, G_x is the gradient in the horizontal direction (along the x-axis), and G_y is the gradient in the vertical direction (along the y-axis).

This approach provides both the strength of the edge (magnitude) and its orientation (direction), making it suitable for wave pattern analysis.

Third, the selection of edges for wave direction measurement is based on a percentile threshold applied to the gradient magnitude. This approach retains only the most significant edges, corresponding to those with the highest sharpness. In this study, the 90th percentile is used to emphasize wave features that exhibit the most distinct and well-defined edges.

Fourth, to further reduce noise while maintaining edges, a median filter with a 5×5 kernel is applied. Median filtering is preferred because it effectively suppresses isolated noise without blurring important structures. A comparison between images with and without median filtering is shown in Fig. 3, highlighting its noise reduction capability.

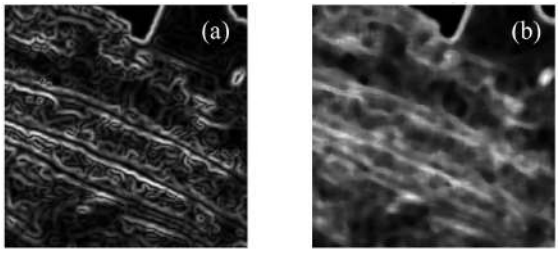

Fig. 3. Comparison of before and after applying median filter: (a) histogram equalization and sobel edge detection applied and (b) histogram equalization and sobel edge detection applied with median filter.

C. Edge Detection and Analysis

Wave crests are symmetrical and introduce a 180° ambiguity in orientation. To resolve this, we apply double-angle averaging, a method that averages orientations in a complex space, as follows.

The gradient directions are averaged using a double-angle approach to resolve directional ambiguity, a common issue in wave pattern analysis.

$$\theta_{\text{wave}} = \frac{1}{2}\arctan\left(\frac{\sum_{x,y}\sin(2\theta_{x,y})}{\sum_{x,y}\cos(2\theta_{x,y})}\right), \tag{5}$$

where $\theta_{x,y}$ is the gradient direction at each pixel, and θ_{wave} is the averaged wave direction derived by resolving the 180° ambiguity using the double-angle trigonometric method.

The final wave direction is determined as orthogonal to the crest direction.

$$\theta_{\text{wave}} = \theta_{\text{crest}} + 90^\circ. \tag{6}$$

This ensures that the wave direction is perpendicular to the detected wave crests.

D. Output Visualization

The final wave direction is visualized by overlaying directional arrows on the satellite image. The step-by-step process of the proposed method, from the original image to the final thresholded edge map, is illustrated in Fig. 4.

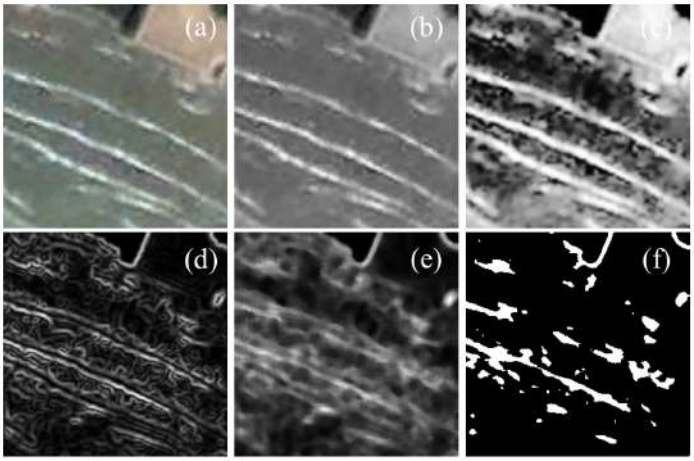

Fig. 4. Sequential visualization of the proposed wave direction estimation process: (a) original image patch, (b) grayscale conversion, (c) histogram equalization, (d) sobel edge detection, (e) median filtering, and (f) thresholding.

Following the complete processing workflow, the final wave direction is displayed by overlaying directional arrows on the satellite image, as shown in Fig. 5. The red arrow indicates the estimated wave direction, while the blue arrow provides a geographic reference for north.

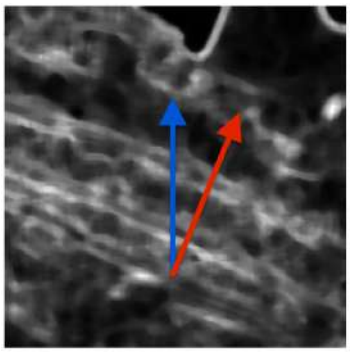

Fig. 5. Visualization of the final wave direction estimation, with directional arrows overlaid on the processed image patch at Chaloem burupha chonlatit road.

IV. EXPERIMENT AND EVALUATION

We evaluated the proposed wave direction estimation method using Sentinel-1 SAR satellite images from coastal regions in Thailand. Two geographically and environmentally distinct sites were selected: Chaloem Burapha Chonlathit Road and Sattahip Beach. These locations were selected as they are recognized as prone areas for coastal erosion. These sites provide 403 and 281 image samples, respectively, with preprocessing steps applied to enhance wave signatures and extract local gradient features [22], [23].

To assess the method's effectiveness, we compared the estimated wave directions against reference annotations derived from expert labeling and auxiliary sources. The performance metrics included the mean absolute error (MAE), the root mean square error (RMSE), directional accuracy which defined as the percentage of predictions within ±15° of the reference, and the number of small flips which is the minor reversals due to 180° ambiguity, common in orientation-based estimation [19], [24].

Experiments were conducted both with and without the median filtering. We further tested three different kernel sizes ($k = 5,\ \ 7$, and 9) to analyze their impact on noise reduction and directional consistency [25].

TABLE I
WAVE DIRECTION PREDICTION METRICS FOR THE CHALOEM BURAPHA CHONLATHIT ROAD SITE.

Model	**MAE (°)**	**RMSE (°)**	**Accuracy within ±15° (%)**	**Small Flips**
No median filter	22.07	28.15	40.40	30
Median filter with $k = 5$	**9.54**	**11.02**	**80.90**	**52**
Median filter with $k = 7$	9.57	11.04	79.70	55
Median filter with $k = 9$	9.71	11.19	77.40	53

TABLE II
WAVE DIRECTION PREDICTION METRICS FOR THE SATTAHIP BEACH SITE.

Model	**MAE (°)**	**RMSE (°)**	**Accuracy within ±15° (%)**	**Small Flips**
No median filter	9.98	12.29	77.60	0
Median filter with $k = 5$	4.28	5.56	98.60	0
Median filter with $k = 7$	**4.23**	**5.47**	**98.90**	0
Median filter with $k = 9$	4.25	5.44	99.30	0

The results clearly show that median filtering substantially improves accuracy and robustness, particularly at Chaloem Burapha, where unfiltered estimates suffered from high error due to environmental noise. A kernel size of $k = 7$ offered the best balance between smoothing and directional detail preservation.

On average, the proposed method achieved a mean absolute error (MAE) of approximately 6.9°, root mean square error (RMSE) of 8.3°, and directional accuracy within ±15° of 89.5% across the tested sites. These results indicate that the method provides reliable and acceptable performance when compared to human expert visual assessment. The performance metrics, particularly when applying a median filter with kernel sizes $k = 5$, 7, and 9, demonstrate a balance between smoothing and preserving directional features, supporting the method's practical applicability for operational coastal monitoring tasks.

V. DISCUSSION

The findings confirm that our approach, which relies on local gradient orientation and double-angle averaging, is a valid and effective technique for estimating wave directions from SAR imagery [19], [23]. The median filter acts as a post-processing step that removes localized noise from land-sea boundaries or other image artifacts without sacrificing wave structure [25].

Although the technique performed well, some estimation flips still occur in areas of weak backscatter or ambiguous orientation, a known limitation in phase-based direction retrieval [26]. These flips may be addressed in future work by integrating auxiliary wind vectors or employing temporal averaging across multiple acquisitions [27].

Another identified limitation is sensitivity to land-sea boundary noise, which often disrupts local gradient calculation. Robust land masking or segmentation strategies should be integrated prior to direction estimation to exclude non-water regions [28].

Though validated on two coastal regions in Thailand, further evaluation across diverse geographies, wave climates, and seasonal variations is essential to assess generalizability.

VI. CONCLUSIONS

This study proposed a wave direction estimation method based on local gradients, Gaussian smoothing, and double-angle orientation averaging. Incorporating a median filter significantly improved directional accuracy, particularly with a kernel size of $k = 7$, which consistently delivered low error and high accuracy.

Experiments on two coastal sites in Thailand demonstrated the method's effectiveness, achieving over 98% directional accuracy in favorable conditions. The method is lightweight, interpretable, and suitable for operational wave monitoring applications.

Future enhancements may include integration of deep learning-based segmentation [28], probabilistic ambiguity resolution models, and hybrid systems combining physical and data-driven approaches [26], [27].

ACKNOWLEDGMENT

The ASEAN IVO project (http://www.nict.go.jp/en/asean ivo/index.html), titled "Coastal Erosion Monitoring Platform Based on Wireless Sensor Networks and 3D Point Clouds from Airborne LiDAR," was involved in the production of the contents of this work and financially supported by NICT (http://www.nict.go.jp/en/index.html).

REFERENCES

[1] E. Bird, *Coastal Geomorphology: An Introduction*. John Wiley & Sons, 2008.

[2] P. Suntra-rachun and A. Buranapratheprat, "Longshore and rip currents during high tide at bangsaen beach, chonburi province," 2017.

[3] J. Phaksopa and P. Sojisuporn, "The analytical of wave characteristics and shoreline changes at tumbon kao roop chang, songkhla province in 2015 and 2016," 2016.

[4] N. Sannatai, S. Ritphring, and S. Prigboonchan, "Shoreline changes along phuket island," 2020.

[5] P. Imlamai, S. Worachananant, and J. Phaksopa, "Monitoring study of coastal morphological change from coastal engineering structures at mrigadayavan palace, phetchaburi province using geo-informatics," 2022.

[6] A. Faiboon and W. Sangmanee, "Geospatial monitoring and forecasts of coastal engineering structures' shoreline transformational impact at songkhla lake mouth," 2022.

[7] W. Truttung, "Study of shoreline change using geographic information system," 2020.

[8] DHI, *Coastal and Offshore Processes*. Danish Hydraulic Institute Manual, 2004.

[9] M. T. Delpey et al., "Wave measurement using buoys: Comparison and analysis of wave buoy data with numerical and remote sensing models," *Ocean Engineering*, vol. 75, pp. 145–156, 2014.

[10] C. A. Hegermiller et al., "Validation of wave direction observations from the coastal hf radar network in southern california," *Journal of Atmospheric and Oceanic Technology*, vol. 33, no. 9, pp. 1927–1941, 2016.

[11] J. Gao et al., "Wave directional spectra retrieval from satellite altimeter data," *Remote Sensing of Environment*, vol. 114, pp. 2123–2134, 2010.

[12] J. Pan et al., "Improving nearshore wave direction estimations using data assimilation techniques," *Coastal Engineering*, vol. 136, pp. 1–13, 2018.

[13] V. Alari et al., "Wind-wave hindcast and validation in the gulf of finland, the baltic sea," *Oceanologia*, vol. 58, no. 2, pp. 88–102, 2016.

[14] A. Luijendijk, G. Hagenaars, R. Ranasinghe, F. Baart, G. Donchyts, and S. Aarninkhof, "The state of the world's beaches," *Scientific Reports*, vol. 8, no. 1, p. 6641, 2018.

[15] Y. Goda, "A comparative review on the functional forms of directional wave spectrum," *Coastal Engineering Journal*, vol. 41, no. 1, pp. 1–20, 1999.

[16] D. E. Hasselmann et al., "Directional wave spectra estimation using the maximum entropy method," *Journal of Atmospheric and Oceanic Technology*, vol. 14, no. 3, pp. 591–598, 1980.

[17] E. Skandali, "Calculation of relative wave direction concerning the vessel's mathematical coordinate system," *Marine Technology Journal*, 2015, Accessed from ResearchGate.

[18] M. Chondros, A. Metallinos, A. Papadimitriou, and V. Tsoukala, "Sediment transport equivalent waves for estimating annually averaged sedimentation and erosion trends in sandy coastal areas," *Journal of Marine Science and Engineering*, vol. 10, no. 11, p. 1726, 2022.

[19] W. Koch, "Directional analysis of sar images aiming at wind direction," *IEEE Transactions on Geoscience and Remote Sensing*, vol. 42, no. 4, pp. 702–710, 2004.

[20] R. C. Gonzalez and R. E. Woods, *Digital Image Processing*. Prentice Hall, 2002.

[21] N. Kanopoulos, N. Vasanthavada, and R. L. Baker, "Design of an image edge detection filter using the sobel operator," *IEEE Journal of Solid-State Circuits*, vol. 23, no. 2, pp. 358–367, 1988. DOI: 10.1109/4.996.

[22] R. Gangeskar, "Wave direction estimation from sentinel-1 sar imagery using azimuthal look and incidence angle features," *Remote Sensing*, vol. 12, no. 12, p. 2016, 2020.

[23] J.-H. Park, S. Kim, and H. Lim, "Sar-based estimation of ocean wave parameters using convolutional neural networks," *Remote Sensing*, vol. 13, no. 7, p. 1285, 2021.

[24] J. A. Johannessen, B. Chapron, F. Collard, et al., "Sar oceanography: Achievements and challenges," *ESA Bulletin*, vol. 123, pp. 100–109, 2005.

[25] L. Gómez and A. Barreira, "Image filtering: Fundamentals and advanced methods," *IEEE Signal Processing Magazine*, vol. 33, no. 4, pp. 89–102, 2016.

[26] C. Ferreira and Y. Simard, "Comparison of methods for wave direction estimation from sar images," *IEEE Transactions on Geoscience and Remote Sensing*, vol. 51, no. 5, pp. 2600–2610, 2013.

[27] W. Alpers and R. Romeiser, "Wind and wave measurements using sar," *Oceanography*, vol. 32, no. 1, pp. 48–57, 2019.

[28] L. Zhao, X. Wang, and Q. Tang, "Deep learning-based sea-land segmentation on sar images for coastal monitoring," *Remote Sensing Letters*, vol. 11, no. 4, pp. 345–354, 2020.